Talay, T. and Erkan, K. (2019). *Xjenza Online*, 7:28–36.

Xjenza Online - Science Journal of the Malta Chamber of Scientists
www.xjenza.org
DOI: 10.7423/XJENZA.2019.1.03

Research Article

Axial Flux Permanent Magnet Motor Design and Optimisation by Using Artificial Neural Networks

Tuğçe Talay[*1] **and Kadir Erkan**[1]
[1] *Yildiz Technical University, Graduate School of Science and Engineering, Mechatronics Engineering, Istanbul, Turkey*

Abstract. In this study, the necessary steps for the design of axial flux permanent magnet motors are shown. The design and analysis of the engine were carried out based on ANSYS Maxwell program. The design parameters of the ANSYS Maxwell program and the artificial neural network system were established in MATLAB, and the most efficient design parameters were found with the trained neural network. The results of the Maxwell program were compared with the results of the artificial neural networks, and optimal working design parameters were found. The most efficient design parameters were submitted to the ANSYS Maxwell 3D design, the cogging torque was subsequently examined and design studies were carried out to reduce the cogging torque.

Keywords: AFPM, ANSYS Maxwell, cogging torque, design optimisation, efficiency, NNTOOL

1 Introduction

Nowadays, electric machines cover 65% of the world's energy consumption. Electric motors are widely used in home appliances, automotive, transportation vehicles, space and aerospace applications.

The increase in demand of these motors has driven many researchers to aim to reach the maximum energy efficiency during their operation.

In particular, there has been an increasing interest in axial flux permanent magnet synchronous motors due to their many advantages, such as compact machine construction with a short frame, high power density and high efficiency. Michael Faraday was the first to design the axial flux engine. In particular, the presence of magnets that provide high magnetic flux, such as neodium (NdFeB) and SmCo, and the reduction in production costs has contributed to the development of permanent magnet motors since the 1980s (Engin & Caner, 2009).

Nowadays, permanent magnet machines are used in many fields, from electric vehicles to space industries. In recent days, the world's leading automobile brands have been operating in the field of electric cars. Due to the high fuel costs and intensive R&D, activities are being carried out to increase the efficiency of the engines of these vehicles.

Firstly, in order to start the design process in electrical machines, design feasibility should be taken into consideration. Hence, presentation of a theoretical design for the perfect electric machine is not sufficient. Therefore, mass production should be thoroughly planned from the first stages of design. In this study, the design of the axial flux permanent magnet motor was created using the ANSYS Maxwell program. For design optimisation, variable ranges were assigned and the performance values were examined, so that an artificial neural network model could be established based on these data. Artificial neural networks can be modelled and learned, and are founded on the neuron structure of the human brain. Artificial neural networks are first trained using existing data and then tested with data not used during training. Although the training process takes time, after this training, the network will have developed a quick decision-making mechanism (Aydin, Zhu, Lipo & Howe, 2007).

The database was developed with various design parameters using the ANSYS Maxwell program, and these data were used in the training and control of artificial neural networks. Detailed design parameter ranges were inputted to the artificial neural network and subsequently compared with the results obtained from Maxwell, in order to determine optimal design parameters.

**Correspondence to*: Tuğçe Talay (tugcetalay2@gmail.com)

In line with the successful results obtained from the artificial neural network, the ANSYS Maxwell program was used to form a three-dimensional machine design, using the best efficient machine parameters. In addition, studies were carried out in order to reduce the impact moment of this machine, thus optimum design parameters were determined and a low-impact, high-efficiency axial intelligent permanent magnet motor design was created.

2 Modelling and Analysis of AFPM by ANSYS Maxwell

The ANSYS Maxwell 3D software package program was used for modelling and analysis of the axial flow permanent magnet motor.

The parametric values used for the starting model are given in Table 1. Here, the values given are the average initial values obtained as a result of a general literature review (Bouaziz, Jaafar & Ammar, 2016; Pahlavani & Gholinejad Omran, 2015; Darmani & Hooshyar, 2015).

The characteristics of the stator used for the analyses in this study consist of 18 slots, eight poles, one rotor, one stator, axial flux, rotor with a disc and permanent magnets placed on the surface. The following table shows the stator, windings, rotor, shaft, permanent magnets and operating conditions in the first selected condition.

Fig. 1 gives the output torque graph of the motor, depending on the position of the rotor in accordance with the selected initial parameters.

An efficiency ratio graph of the motor, depending on the position of the rotor in accordance with the selected initial parameters is given in Fig. 2.

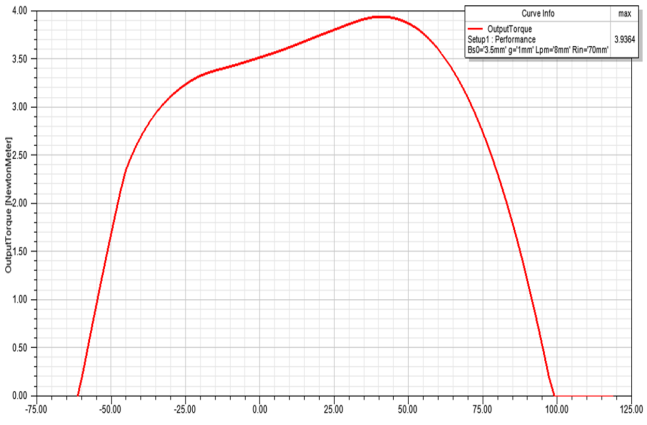

Figure 1: Output torque graph according to rotor position.

Table 1: Parameters of reference AFPM Machine.

	Parameter	Values
Machine	Source Type	DC
	Structure	Axial-Flux Rotor
	Stator Type	AXIAL_AC
	Rotor Type	AXIAL_PM
	Air Gap Length (mm)	1
	Parameter	**Values**
Stator	Number of Poles	8
	Number of Slots	18
	Outer Diameter (mm)	120
	Inner Diameter (mm)	70
	Length (mm)	25
	Stacking Factor	0.95
	Steel Type	D23_50
Hs0 = 0.1 (mm) Hs2 = 4.5 (mm) Bs0 = 3.5 (mm) Bs1 = 6.0 (mm) Bs2 = 6.0 (mm)	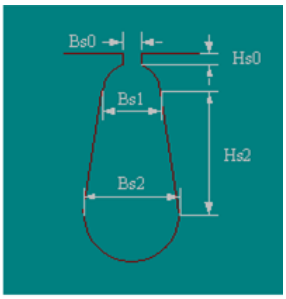	
	Parameter	**Values**
Winding	Winding Layers	2
	Parallel Branches	1
	Conductor per Slots	170
	Coil Pitch	1
	Number of Strands	2
	Wire Wrap	0
	Wire Size (mm)	0.269
	Parameter	**Values**
Rotor	Number of Poles	8
	Skew Width (deg)	0
	Outer Diameter (mm)	120
	Inner Diameter(mm)	70
	Length (mm)	25
	Stacking Factor	0.95
	Steel Type	D23_50
	Parameter	**Values**
PM	Embrace	0.7
	Magnet Type	XG96/40
	Magnet Length (mm)	25
	Magnet Thickness (mm)	8
	Parameter	**Values**
Shaft	Frictional Loss (W)	12
	Windage Loss (W)	12
	Reference Speed (rpm)	3000
	Parameter	**Values**
Working Conditions	Rated Output Power (W)	500
	Rated Voltage (V)	220
	Rated Speed (rpm)	1500
	Operating Temp. (cel)	75

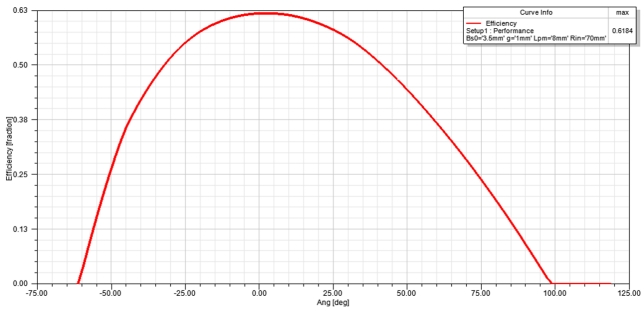

Figure 2: Efficiency ratio graph according to rotor position.

3 Determination and Optimisation of Variable Parameters of AFPM

Inspired by a genetic algorithm method to increase the efficiency of AFPM, design variables and the results of crossing these variable design parameters will be evaluated.

The main design parameters affecting the efficiency are air gap (g), stator slot opening (Bs0), inner diameter of the rotor (Rin), and permanent magnet thickness (Lpm). One of the most important design parameters is λ, which is the result of dividing the motor inner diameter by the motor outer diameter (Di / Do). By choosing rotor initial diameter (Rin) as a design variable, λ will also be affected proportionally. Design values are assigned as Fig. 3 in Maxwell's "optimectrics" tab.

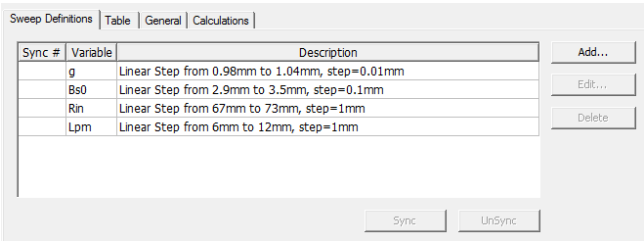

Figure 3: Variable design parameter.

As a result of the analysis, which takes about two days, 2401 data were obtained. The 2401 design parameters obtained were recorded in order to be used in the training and control of artificial neural networks.

4 Structure of the Artificial Neural Network

In this study, input data were generated by randomly selecting 427 of the design data produced in the ANSYS Maxwell program. Selected parameters were as follows: air gap (g), stator slot opening (Bs0), inner diameter of the rotor (Rin), permanent magnet thickness (Lpm), and their combinations.

The output data refers to the efficiency ratio of the values that are formed as a result of the design combination of these parameters.

In the training of the network, the back-propagation algorithm was used, thus the fault will be spread from outer layer to lower layers. Tangent-Sigmoid function was used for transfer function. The structure of the Artificial Neural Network is given in Fig. 4.

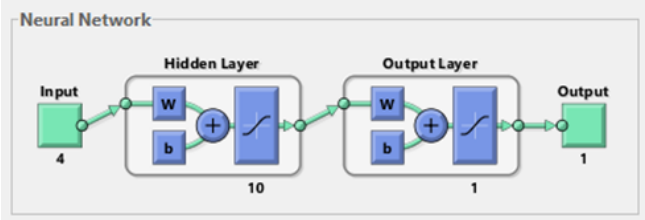

Figure 4: Structure of Artificial Neural Network.

4.1 Performance of the Artificial Neural Network

The neural network reached best validation performance at 35 epochs. In Fig. 5, the mean squared error histogram for training, test, and validation data is shown.

4.2 Regression Results of the Artificial Neural Network

In the study, the artificial neural network (ANN) method was used to find the regression value (correlation factor) between the target values and the calculated values, which was recorded between 0.9995 and 0.9996.

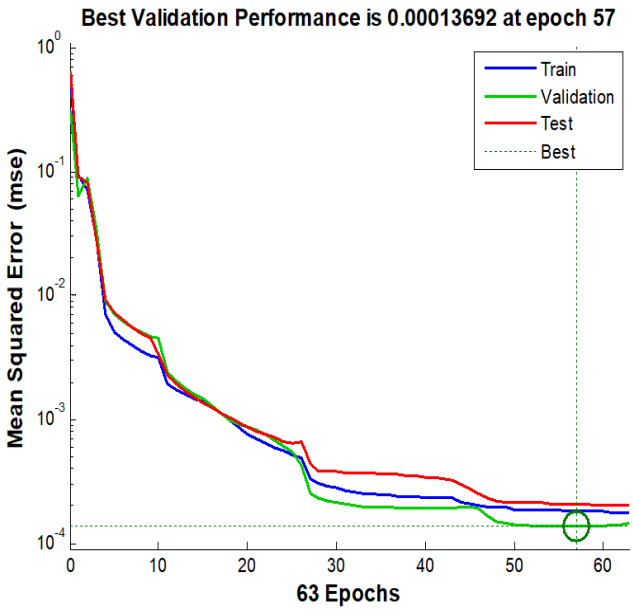

Figure 5: Performance of artificial neural network (main squared error).

The results obtained from the study show that the ANN method can be used successfully. The regression Values for Training, Test, Validation and All data are given in Fig. 6.

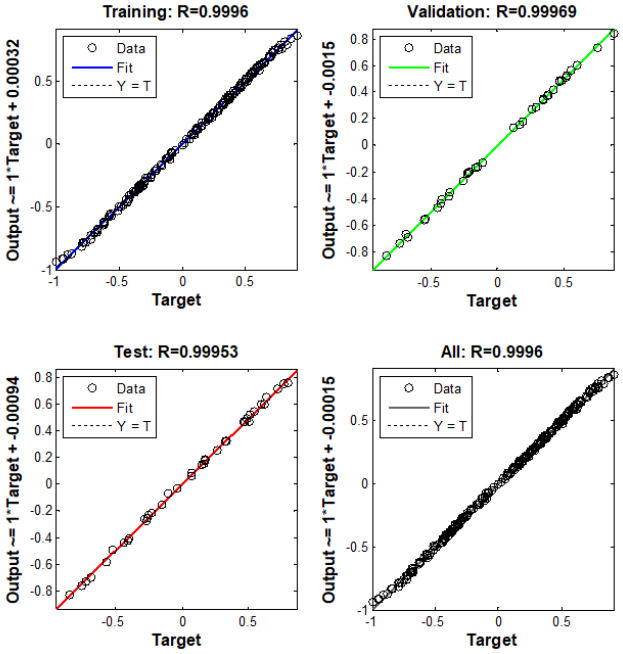

Figure 6: Regression Values for Training, Test, Validation and All.

4.3 Application of the Artificial Neural Network

According to ANN performance results, the training is completed without reaching the number of iterations entered. Our verification and test data are in parallel with the training data, proving that the network has learnt the process successfully. Therefore, network1 is ready to be exported into NNTOOL and simulated.

After proving that the artificial neural network was successfully working (tested and approved 427 pcs data), the aim was to obtain the highest efficiency motor by gathering efficiency ratio results for the different parameter values.

We used 427 of the 2041 data obtained from ANSY Maxwell for the training of the network. Subsequently, 133 different parameter combinations were chosen from the remaining data, so that the performance of the trained network and the amount of error could be investigated.

The selected design parameters were run in the trained network1 and the efficiency ratio values were thus predicted by the artificial neural network. The estimated efficiency ratio values recorded from the artificial neural network were compared to target values which were obtained from ANSYS Maxwell. Referring

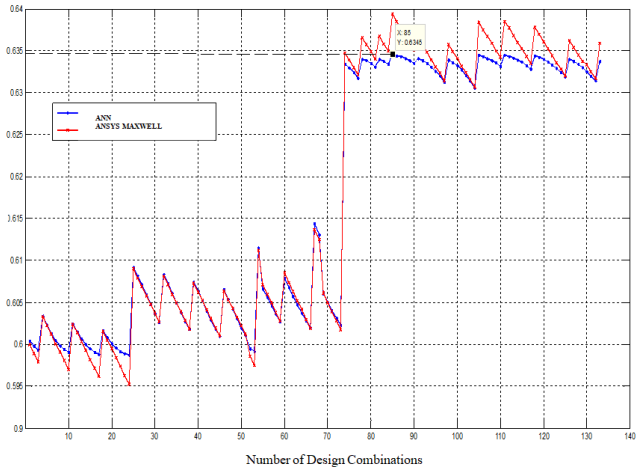

Figure 7: Target efficiency ratio vs. predicted ANN results (ANN predicted maximum efficiency ratio is marked).

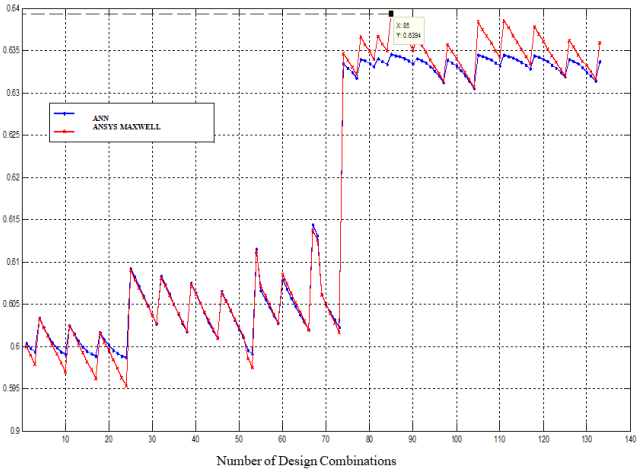

Figure 8: Target efficiency ratio vs. predicted ANN results (Target of maximum efficiency ratio is marked).

to Figs. 7 and 8, the target values from ANSYS Maxwell are parallel with the predicted values from the neural network. This proves that the trained network can be used for the design optimisations, as it confirms that the training process was completed successfully for different design values.

The results obtained from Maxwell in the artificial neural network reached the highest efficiency in the combination of parameters in design 85. According to these results, the 85th design parameters provide the highest efficiency. The 85th design parameters are shown in Table 2.

Table 2: Optimised design parameters.

Bs0 (mm)	G (mm)	Lpm (mm)	Rin (mm)
3	0.98	12	73

The efficiency, torque and losses of ANSYS Maxwell, which are optimised by artificial neural networks, were compared, and the design results of the initial stage were also compared with that of the optimised design results.

The efficiency increased by 2.05% compared to the initial stage. Total losses decreased by 28.66 Watts. Maximum output torque increased by 0.1024 N m. Initial value and optimized comparison are given in Table 3.

Table 3: Initial value and optimised design comparison.

	Initial Value	Optimised Value
Efficiency (%):	61.7592	63.8116
Maximum Torque (N m):	3.9364	4.0388
Total Loss (W):	340.552	311.892

Initial torque value and optimized torque comparison is given in Fig. 9. Initial state efficiency and optimized efficiency ratio comparison is given in Fig. 10.

The optimisation of the axial flow of permanent magnet motor in ANSYS Maxwell are the parameters that give the highest efficiency in the selected range. Using these parameters, the design of the engine was submitted to ANSYS Maxwell three-dimensional machine design.

5 3-D Design Modelling of Axial Flux Permanent Magnet Machine by ANSYS Maxwell

After analysing and modelling in Maxwell rmexport, the design was submitted to Maxwell3DDesign. In Fig. 11, a half-model three-dimensional axial intelligent permanent magnet machine is shown.

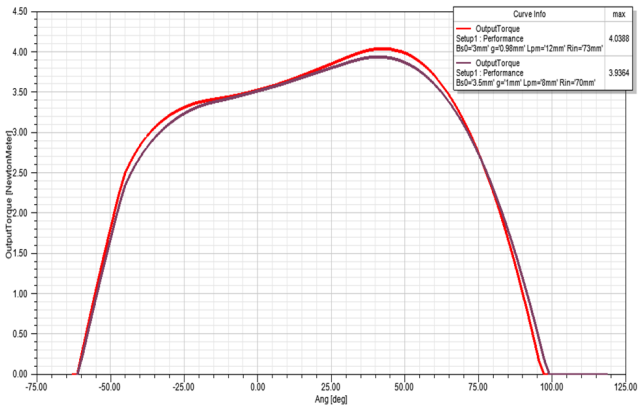

Figure 9: According to rotor position, initial state and optimised torque comparison.

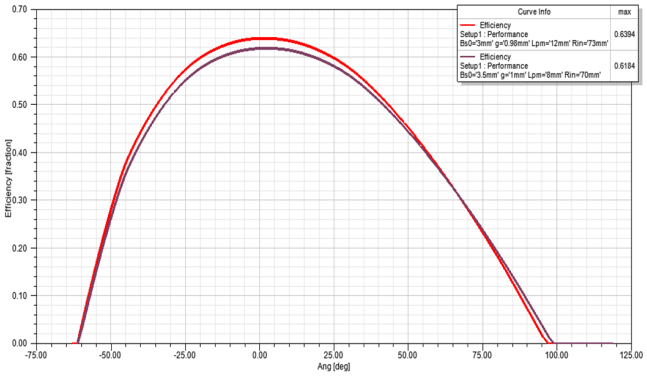

Figure 10: According to rotor position, initial state and optimised efficiency ratio comparison.

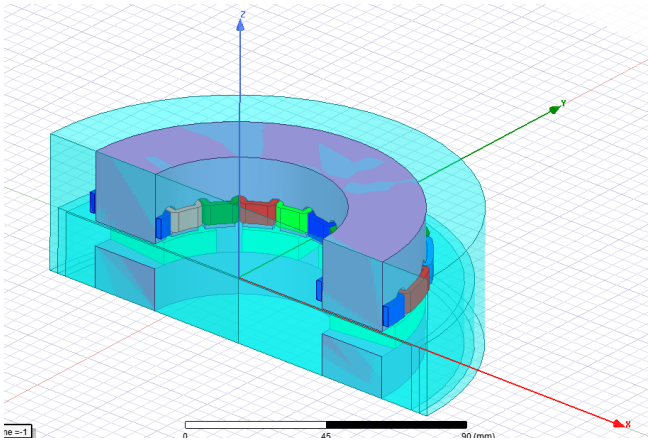

Figure 11: Half-model of permanent magnet motor with axial flow.

6 Calculation of Cogging Torque

Cogging torque is the reluctance moment of the motor due to its magnetic flux and reluctance. This moment is examined structurally and has a negative effect on nominal torque in the operation of the motor. In the simulation of the permanent magnet axial flow motor with ANSYS Maxwell program, different settings must be made in each step. In the calculation of the moment of torque, the motor needs to be moved with mechanical steps (Ayçiçek, Bekiroğlu, Senol & Oner, 2015). For a higher resolution, this setting can be arranged optionally. Cogging Torque in the initial stage values are given in Fig. 12.

7 Cogging Torque Reducing Techniques of AFPM

Minimising cogging torque in designing axial-flux permanent-magnet (AFPM) motors is one of the important issues which must be considered during the design process, as it leads to output torque ripple, vibrations and noise (Kumar & Srivastava, 2018a). There are a variety of techniques that exist for minimising the

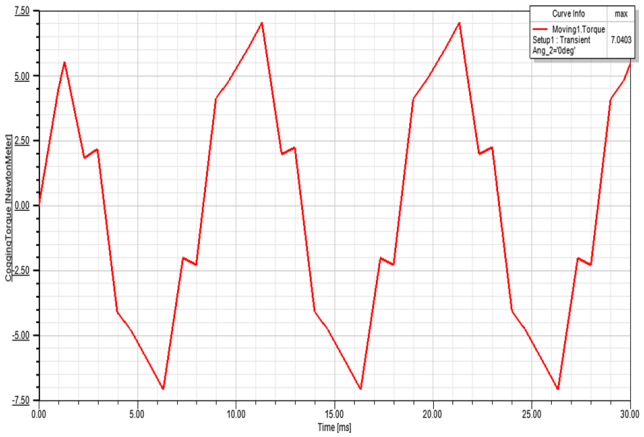

Figure 12: Cogging Torque in the initial stage.

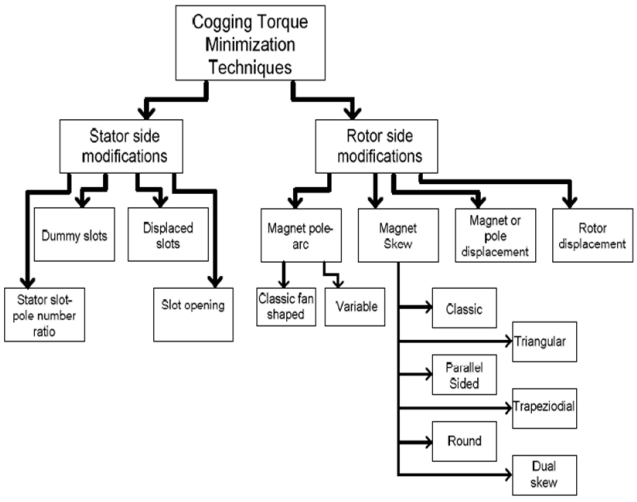

Figure 13: Summary of cogging torque minimisation techniques for AFPM machines (Aydin, 2008).

cogging torque (Bianchini, Immovilli, Bellini & Davoli, 2012). Out of these, the various rotor modification techniques are directly applicable to axial flux machines. However, the stator modification techniques cannot be directly applied, due to difficulty in punching slots in axial stator laminations, leading to high cost (Kumar & Srivastava, 2018a). In general, cogging torque minimisation in AFPM machines can be considered in two manners: modifications from the stator side and rotor side. Summary of cogging torque minimization techniques for AFPM machines are given in Fig. 13.

7.1 Stator Side Modifications

There are some minimisation techniques which can be applied for the stator side, such as dummy slots in stator teeth, ratio of stator slot number to rotor pole number, slot openings and displaced slots (Aydin, 2008).

It is known that cogging torque is produced by the interaction between the edges of the magnet poles and the stator slots. By introducing dummy slots in the stator teeth, the interaction between magnets and stator slots will be increased, thus increasing the main frequency, removing some of the harmonic orders, and reducing the maximum amount of cogging torque. This method can even cause saturation on teeth surface by changing the distribution of flux lines (Bianchini et al., 2012). The dummy slots are not as deep as the slots where windings are positioned, but if feasible, for cogging torque mitigation, small notches in the teeth are sufficient (Ferreira, Leite & Costa, 2015). Due to the high number of poles and consequently, slots required, the width of the teeth would not be enough to accommodate the notches in low speed applications (Ferreira et al., 2015). Furthermore, these methods are not practical and they are high cost solutions for AFPM machines.

One of the cogging torque minimisation methods used in the stator, was to arrange the ratio of stator slot number to pole number. However, in fractional slot machines, the rotor magnets have different positions according to the stator slots, hence generating the cogging torque components which are out of phase refer to each other, are partially cancelled (Aydin, 2008). In axial flux machines, the stator laminations are spirally wound and thus, cutting of slots is difficult. Therefore, its customised design for cogging reduction is far more complex and not practical, as the design cost is high (Kumar & Srivastava, 2018b).

Due to reasons previously mentioned, the axial fluxes we designed were analysed with a focus on rotor side modifications, in order to reduce the impact of the cogging torque.

7.2 Rotor Side Modifications

For AFPM motors, it is more important to work on techniques that will reduce the cogging torque on the rotor side, rather than stator side techniques. This is due to the fact that the motor structure is axial and thus, the modifications required on the rotor are more practical, cost less and are easier to design.

These methods include: magnet shaping, optimising magnet pole arc to pole pitch ratio, pole arc offset, narrowing rotor pole embrace, pole-slot combination, magnet skewing, etc. (Kumar & Srivastava, 2018b). As a result of rotor shifting technology, the rotor torque is reduced at the appropriate angle. Magnet skewing technique is a method in which one side of the magnet is attached to the other side of the magnet; results are based on the production of the magnet according to the resulting new shape. The magnet or pole shift (grouping technique) is the shifting of the adjacent magnets in relation to each other.

7.2.1 Cogging Torque Minimisation by Magnet Pole-Arc to Pole-Pitch Ratio

Cogging torque is being triggering by the interaction between the edges of the magnet poles and the stator slots. Magnet pole-arc is an important topic because both the magnitude and shape of the cogging torque waveform depend on the magnet pole-arc (Aydin, 2008). The magnet leakage flux can be reduced by decreasing the magnet pole-arc to pole pitch ratio, however, this also reduces the magnetic flux and consequently, the average torque (Aydin, 2008). An AFPM rotor with two different magnet steps is shown in Fig. 14. Cogging Torque optimized values after Magnet Pole-Arc to Pole-Pitch Ratio technique are given in Fig. 15.

7.2.2 Cogging Torque Minimisation by Magnet Skew

One of the most efficient methods to reduce cogging torque is Magnet skewing for AFPM machines, because this modification can be implemented quickly with ease. Magnet skewing is generally used for conventional permanent magnet motors, as well as AFPM motors (Güleç, Yolaçan, Demir, Ocak & Aydin, 2016). As shown in Fig. 16, the location of the direct axis of the magnet shifts gradually in peripheral direction, as it is traced from inner radius to outer radius of the rotor core (Reza & Srivastava, 2018). The machine is divided into a certain number of annular slices in the radial direction. The direct axis of each slice is displaced by a certain angle (θs) (Reza & Srivastava, 2018).

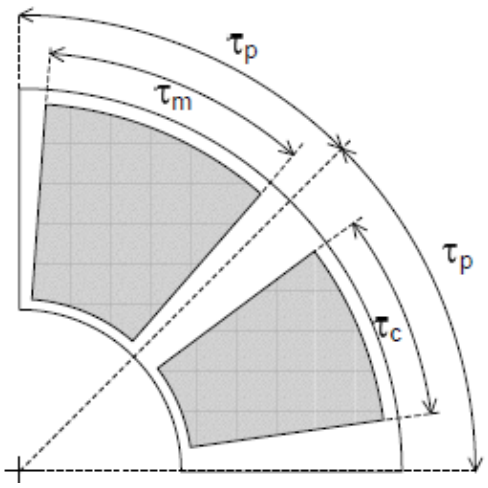

Figure 14: An AFPM rotor with two different magnet steps.

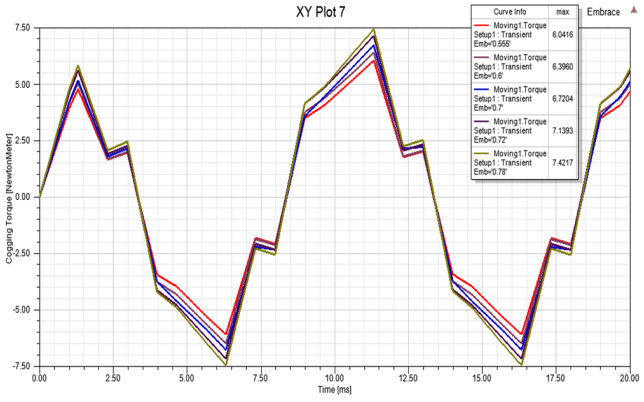

Figure 15: Cogging Torque minimisation after Magnet Pole-Arc to Pole-Pitch Ratio technique.

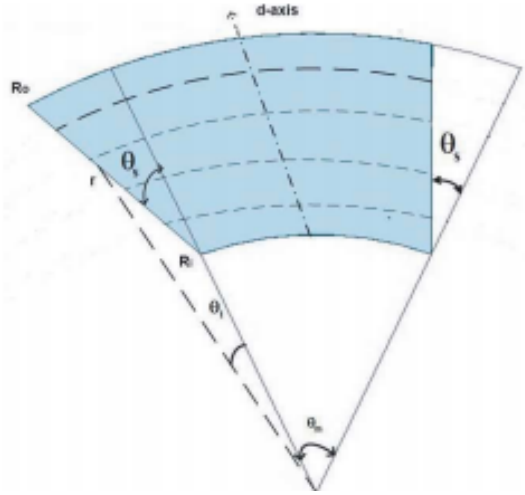

Figure 16: Rotor structure with skewed magnet (Reza & Srivastava, 2018).

Different registration techniques are available for AFPM motors. These techniques include conventional magnet skew, triangular magnet skew, parallel-sided magnets, trapezoidal magnet skew, circular magnets and dual skewed magnets. Such methods are just some of the low-cost techniques that can be applied to the rotor side of the permanent magnet disc motors. Cogging Torque minimized values following application of the skewing technique, are shown in Fig. 17.

7.2.3 Cogging Torque Minimisation by Rotor Displacement

In dual air-gap AFPM motors, the cogging torque is equal to the vector sum of the cogging torques in each air gap. Therefore, if one of the rotors is rotated relative to the other, the peak value of the total cogging torque can be pulled down, since the vector sum of the cogging torque in each air gap will give the total cogging torque (Ayçiçek, 2012). Fig. 18 shows the comparison between two different AFPM motor's rotor displacement. Cogging Torque minimized values are shown in Fig. 19 after rotor displacement technique.

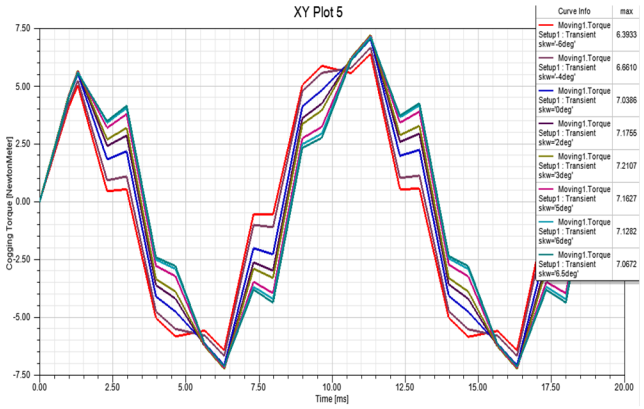

Figure 17: Cogging Torque minimisation after skewing technique.

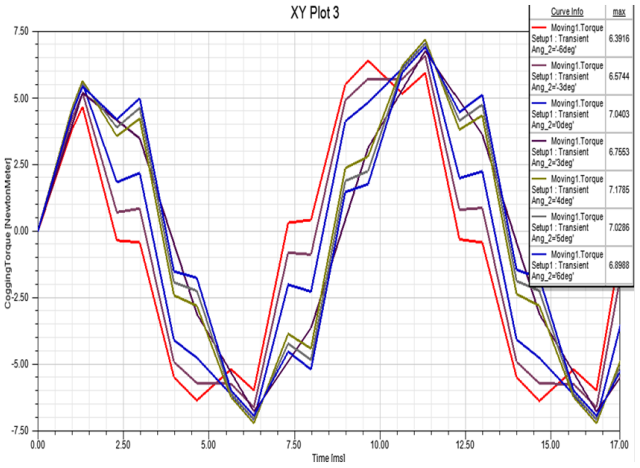

Figure 19: Cogging Torque minimisation after rotor displacement technique.

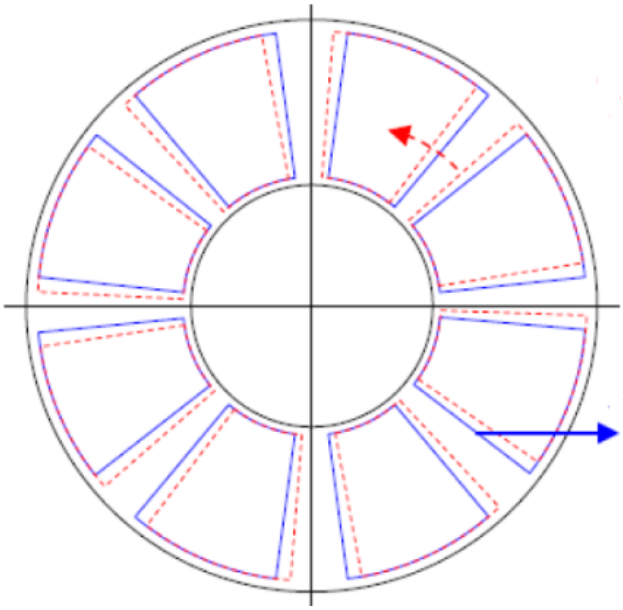

Figure 18: Comparison of two different AFPM motor's rotor displacement (Aydin, Zhu, Lipo & Howe, 2007).

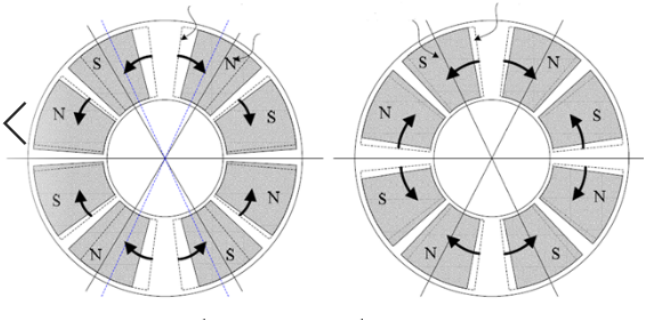

Figure 20: Magnet placement (pole displacement) options of AFPM motors (Aydin, Zhu, Lipo & Howe, 2007).

7.2.4 Magnet or Pole Displacement (Grouping Technique)

Another effective method for cogging torque minimisation is to slide adjacent magnets relative to each other, as shown in Fig. 20. However, when the magnets are shifted from their symmetrical position, the leakage flux on one side of the magnet will increase, whilst the leakage flux on the other side will decrease. Another disadvantage of this method is that it causes distortion of the counter electromotive force waveform and the moment fluctuation (Aydin et al., 2007).

8 Conclusions

In this paper, an artificial neural network-based design optimisation algorithm for an AFPM motor was proposed. The design variables were varied, and the subsequent effects on performance indices were studied by performing ANSYS Maxwell. Having obtained discrete data from ANSYS Maxwell, NNTOOL was used for training the data and further optimisation. The results of the network disclosed an optimised AFPM motor design.

The trained network was used to validate the artificial neural network-based design solution. Results from the artificial neural network prove the precision of the design variables by getting maximum effective design solution at the same design variables with ANSYS Maxwell data by using artificial neural network. We analysed so many design data in a very short time and the design variables which gives maximum efficiency, has been found. With the artificial neural network design solution, we were able to increase efficiency by 2.05% and the maximum output torque by 0.1024 N m compared to the initial stage design.

For AFPM, cogging torque is crucial as it needs to be reduced to improve the design optimisation. In this study, various cogging torque minimisation techniques for AFPM machines were reviewed. It is evident that there are a range of different techniques which are applicable for AFPM machines and can be used to reduce the cogging torque. Due to the complexity and cost of stator manufacturing, this study focussed on rotor side minimisation techniques. Results showed that adjustment of Magnet Pole-Arc to Pole-Pitch Ratio resulted in reduction of cogging torque by 10.1%, that the magnet skewing technique produced a 9.17% decrease and that following rotor displacement, cogging torque decreased by 9.2%, compared to initial structure.

References

Ayçiçek, E. (2012). *Design of Axial Flux Permanent Magnet Synchronous Motor with Reduced Cogging Torque* (Doctoral dissertation, Yildiz Technical University, Institute of Science, Technology, Department of Electrical and Electronics Engineering, Istanbul, Turkey).

Ayçiçek, E., Bekiroğlu, N., Senol, I. & Oner, Y. (2015). Rotor Configuration for Cogging Torque Minimization of the Open- Slot Structured Axial Flux Permanent Magnet Synchronous Motors. *Appl. Comput. Electromagn. Soc. J. 30*(4), 396–408.

Aydin, M. (2008). Magnet Skew in Cogging Torque Minimization of Axial Gap Permanent Magnet. In *2008 18th International Conference on Electrical Machines*. Vilamoura, Portugal: IEEE.

Aydin, M., Zhu, Z. Q., Lipo, T. A. & Howe, D. (2007). Minimization of cogging torque in axial-flux permanent-magnet machines: Design concepts. *IEEE Trans. Magn. 43*(9), 3614–3622.

Bianchini, C., Immovilli, F., Bellini, A. & Davoli, M. (2012). Review of design solutions for internal permanent-magnet machines cogging torque reduction. *IEEE Trans. Magn. 48*(10), 2685–2693.

Bouaziz, O., Jaafar, I. & Ammar, F. B. (2016). 3D Finite Element Modelling of Single-Sided Axial-Flux Permanent-Magnet Synchronous Machine. In *3rd International Conference on Automation, Control, Engineering and Computer Science (ACECS'16)* (Vol. Proceedings of Engineering & Technology (PET), pp. 669–674). Hammamet, Tunisia.

Darmani, M. A. & Hooshyar, H. (2015). Optimal Design of Axial Flux Permanent Magnet Synchronous Motor for Electric Vehicle Applications Using GA and FEM. *J. Electr. Comput. Eng. Innov. 3*(2), 89–97.

Engin, H. & Caner, A. (2009). An Overview Control Methode of Axial Flux Motors. In *5. Uluslararasi ileri Teknolojiler Sempozyumu (IATS'09), 13–15 Mayis 2009* (Vol. IATS'09). Karabük, Turkey.

Ferreira, A. P., Leite, A. V. & Costa, A. F. (2015). Comprehensive Analysis and Evaluation of Cogging Torque in Axial Flux Permanent Magnet Machines. In *2015 IEEE 10th International Symposium on Diagnostics for Electrical Machines, Power Electronics and Drives (SDEMPED)*. Guarda, Portugal: IEEE.

Güleç, M., Yolaçan, E., Demir, Y., Ocak, O. & Aydin, M. (2016). Modeling based on 3D finite element analysis and experimental study of a 24-slot 8-pole axial-flux permanent-magnet synchronous motor for no cogging torque and sinusoidal back-EMF. *Turkish J. Electr. Eng. Comput. Sci. 24*(1), 262–275.

Kumar, P. & Srivastava, R. K. (2018a). Cost-Effective Stator Modification Techniques for Cogging Torque Reduction in Axial Flux Permanent Magnet Machines. In *2018 IEEE Transportation Electrification Conference and Expo, Asia-Pacific (ITEC Asia-Pacific)*. Bangkok, Thailand: IEEE.

Kumar, P. & Srivastava, R. K. (2018b). Influence of Rotor Magnet Shapes on Performance of Axial Flux Permanent Magnet Machines. *Prog. Electromagn. Res. C*, *85*, 155–165.

Pahlavani, M. A. & Gholinejad Omran, H. R. (2015). A New Analytical Description and FEA Validation of an Effective Method to Reduce the Cogging Torque in SM-AFPM Motors. *Prog. Electromagn. Res. M*, *42*, 189–197.

Reza, M. M. & Srivastava, R. K. (2018). Semi-Analytical Model for Skewed Magnet Axial Flux Machine. *Prog. Electromagn. Res. M*, *68*, 109–117.